Spectrometry of cosmic-ray neutrons with HENSA during a minimum of solar activity in 2020

Nil Mont Geli (UPC)
nil.mont@upc.edu

Álvaro Quero Ballesterors (UGR)
alvarojquero21@ugr.es

Ariel Tarifeño Saldivia (IFIC)
atarisal@ific.uv.es

HENSA
High Efficiency Neutron Spectrometry Array

http://www.hensaproject.org

UNIVERSIDAD DE GRANADA
IFIC INSTITUT DE FÍSICA CORPUSCULAR
CSIC CONSEJO SUPERIOR DE INVESTIGACIONES CIENTÍFICAS
UNIVERSITAT POLITÈCNICA DE CATALUNYA BARCELONATECH

The origin of cosmic-ray neutrons

- Primary cosmic-rays are mainly composed of protons & He nuclei.
- Neutrons are produced as secondary particles in Extensive Air Showers (minimum energy ~500 MeV).
- Sources: SEP, Galactic & extra-galactic cosmic-rays.

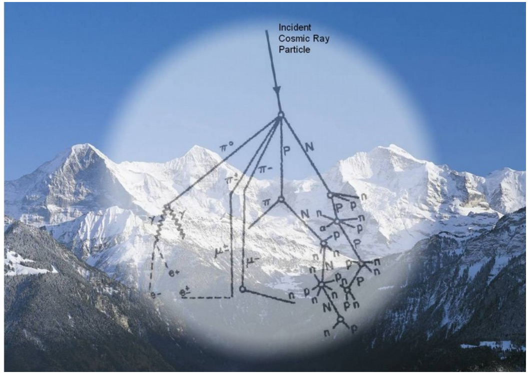

Schema: Simpson et al. (1953, Phys. Review 90, 934)

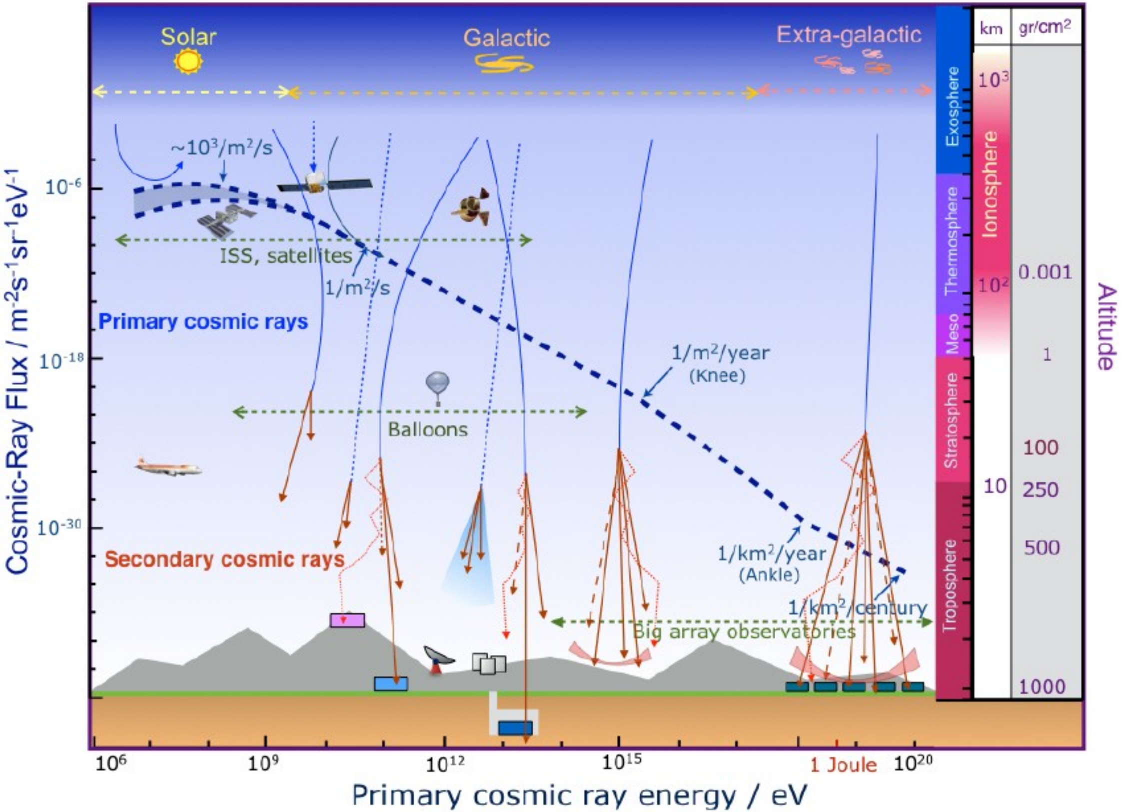

Credits Tragaldabas Collaboration

Instrumentation networks on Earth for secondary cosmic-rays

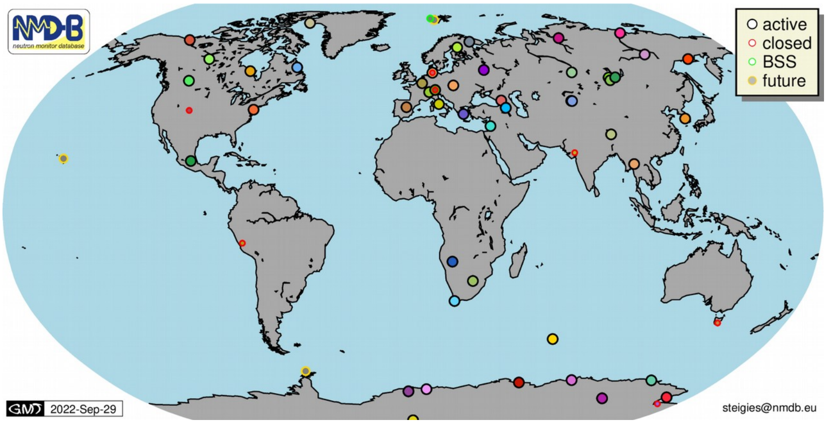

- Examples of ground-based detectors can be **neutron monitors** or **muon detectors**.

- The Neutron Monitor Database (**NMDB**) offers real-time global data from multiple neutron monitor stations, but these detectors **lack spectral resolution**.

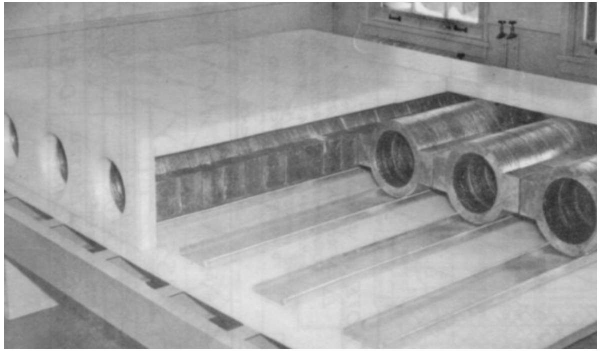

Standard neutron monitor (NM64): BF3 Tube + Polyethylene + Pb Layers

Cosmic-rays flux is affected by the geomagnetic latitude.

$$R = \frac{pc}{|q|} = \frac{pc}{Ze} = r_L|\vec{B}|c$$

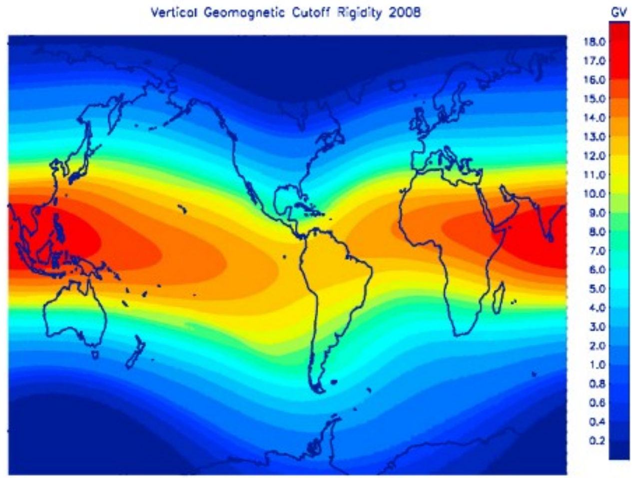

Why is it important to characterize the cosmic neutron spectrum?

We aim to **characterize the secondary cosmic-ray neutron flux magnitude and spectrum** for:

Space weather applications

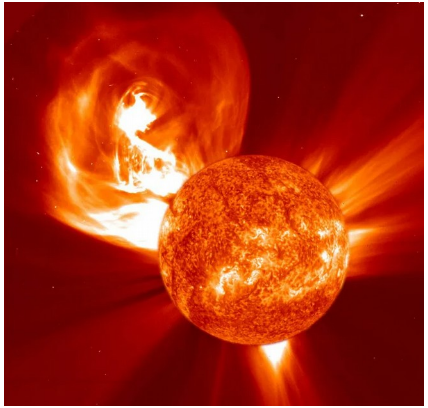

Image of a CME from the NASA webiste

Determination of the neutron ambient dose

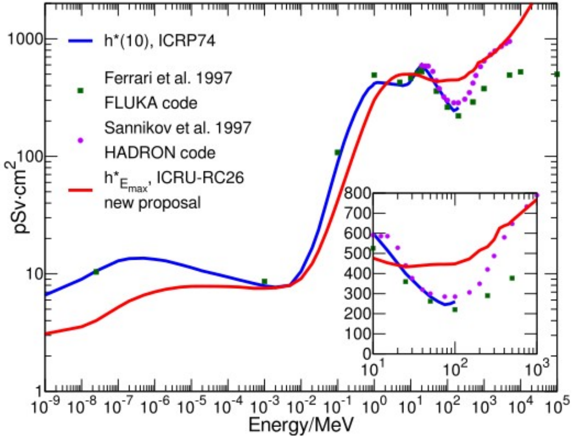

Neutron to dose conversion coefficients

Analysis of Single Events in Microelectronics

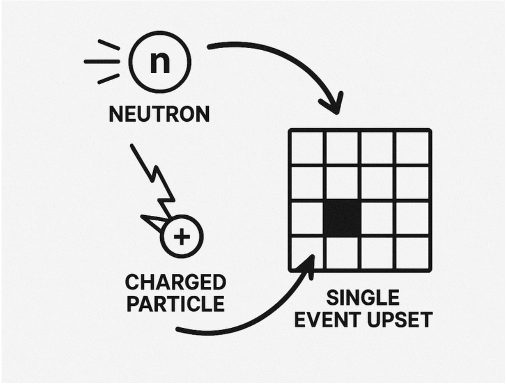

Schema of a Single Event Upset (SEU) produced by a neutron

The anti-correlation between neutron flux and solar activity

Solar activity induces a modulation in the flux of galactic cosmic-rays

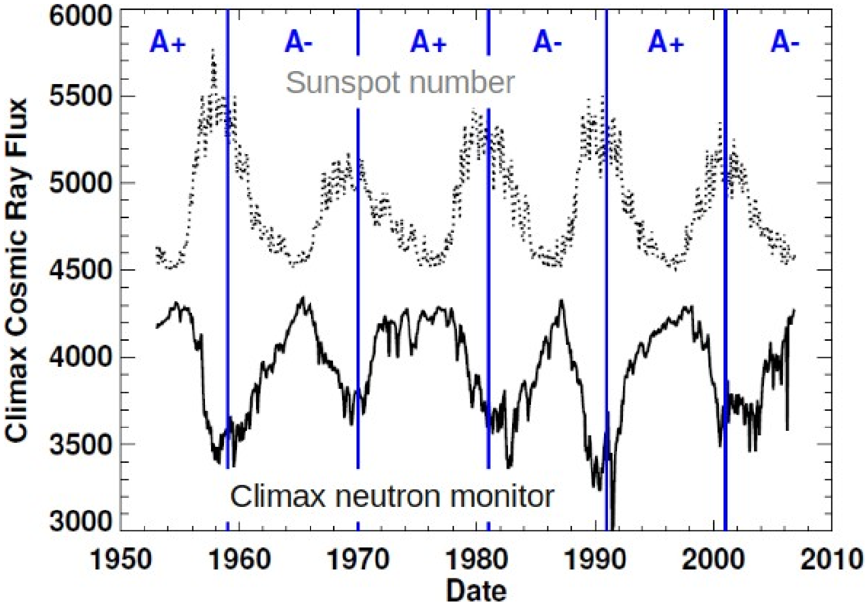

Neutron background anti-correlation with solar cycle. Cosmic Ray flux from the Climax Neutron Monitor and rescaled Sunspot Number.

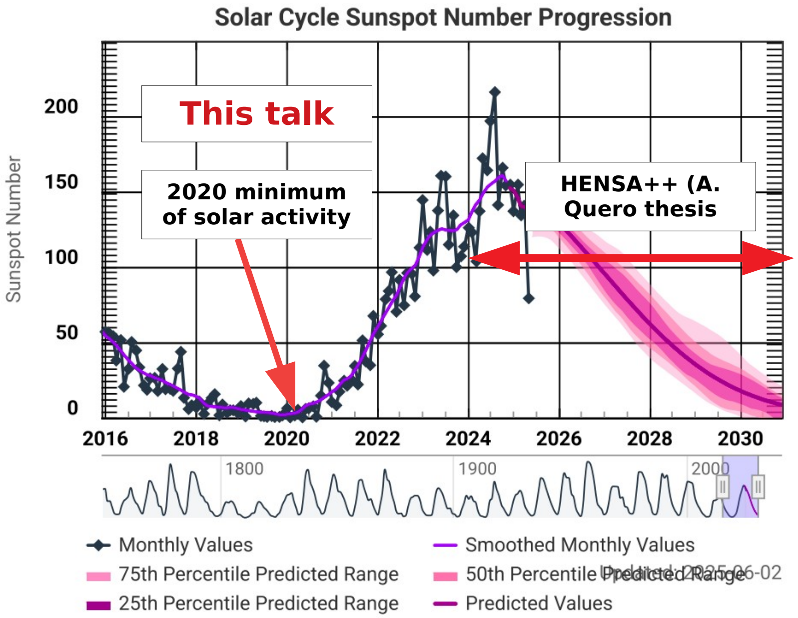

NOAA/NASA forecast for Solar Cycle 25. Updated on 30/06/2025.

The anti-correlation between neutron flux and solar activity

Solar activity induces a modulation in the flux of galactic cosmic-rays

The 2020 campign provides the “baseline” for future studies of solar activity impact on cosmic-rays neutrons spectrum

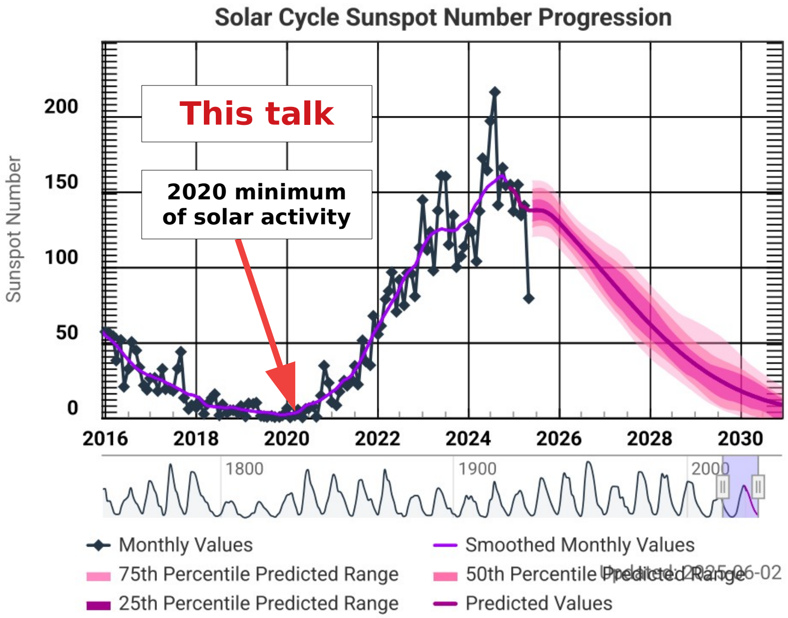

NOAA/NASA forecast for Solar Cycle 25. Updated on 30/06/2025.

How do we perform neutron spectrometry?

- **Detection principle** (Bonner Sphere Spectrometers):

Counter with high sensitivity to thermal neutrons + Materials with a good moderation-capture ratio and metal converters → Sensitivity from thermal to GeV neutrons

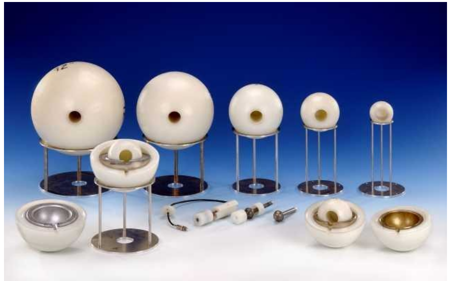

NEMUS Bonner Spheres System

- **Spectrum reconstruction**:

Unfolding algorithm

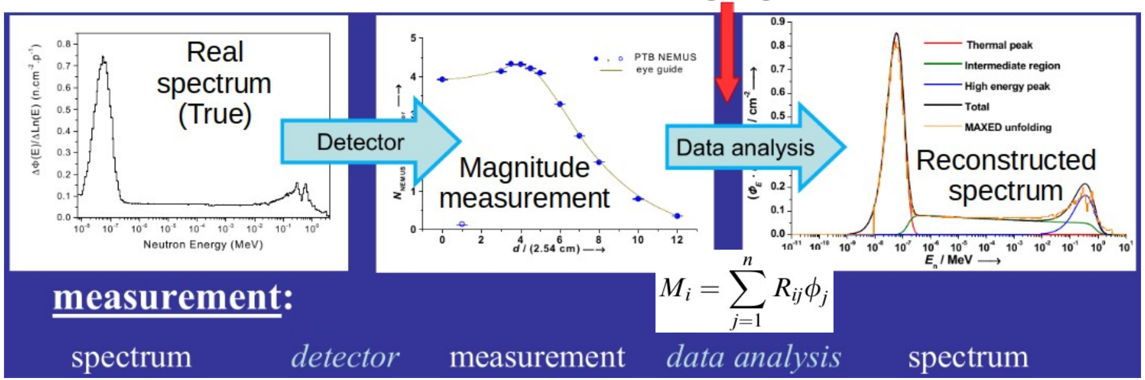

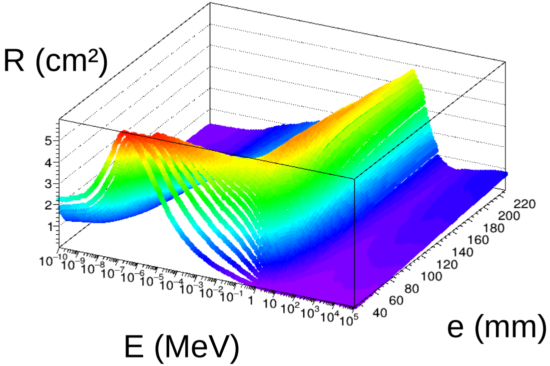

The HENSA project

http://www.hensaproject.org

HENSA High Efficiency Neutron Spectrometry Array

- Development and application of high-efficiency neutron spectrometers
- Based on Bonner Sphere Spectrometers (BSS).
- Topology modification to increase detection efficiency (5% - 15%). Typical BSS doesn't have enough efficiency to resolve the neutron spectrum within short time intervals.
- Energy sensitivity from meV to GeV neutrons, complementing the information of NMDB.
- Main applications: Space weather, cosmic-ray physics, ambient dosimetry, underground.

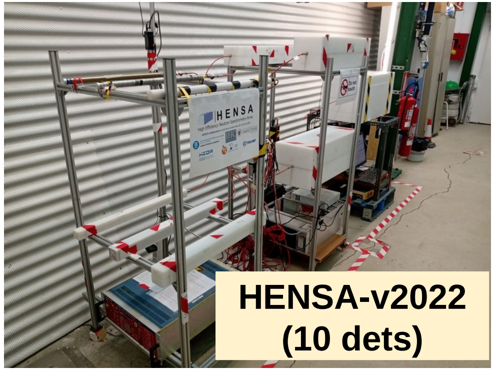

HENSA-v2020 at LSC (2021 - 2025)

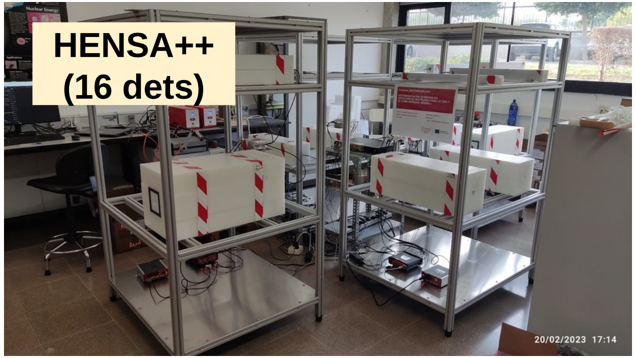

The HENSA++ spectrometer (2024)

HENSA-v2019

Setup for this talk

HENSA
High Efficiency Neutron Spectrometry Array

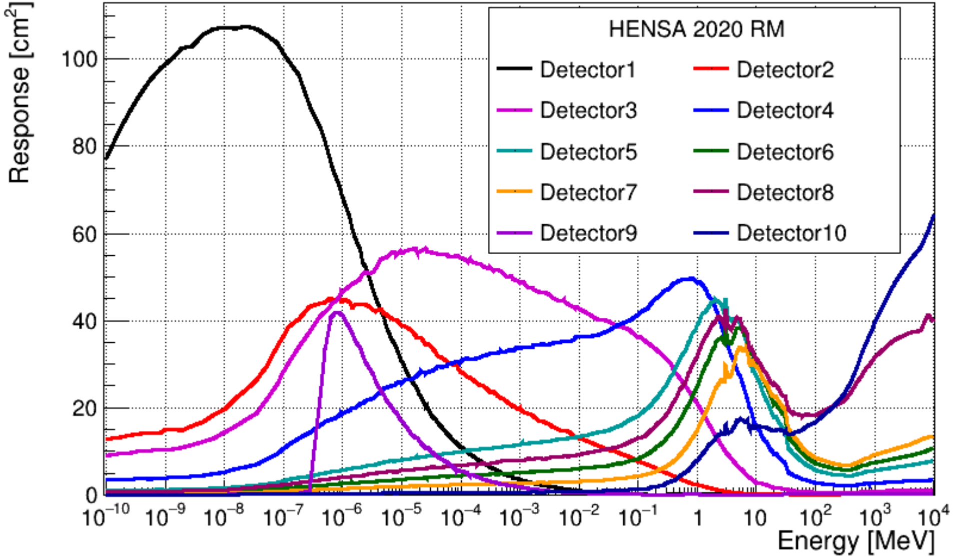

The 2020 CR campaign

HENSA campaign along the Spanish territory close to the minimum of solar activity (2020, solar cycle #25)

Cosmic ray induced neutron background
+ Cosmic ray physics and space weather
+ Environmental radiation dosimetry
+ Single-event upsets in microelectronics

www.hensaproject.org

HENSA
High Efficiency Neutron Spectrometry Array

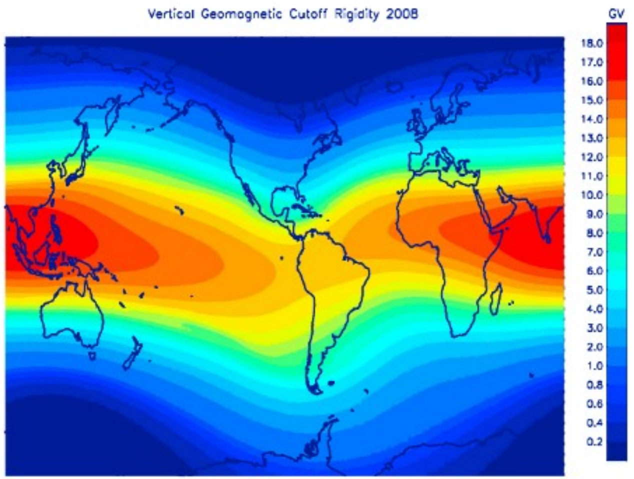

Neutrons produced by cosmic rays depends on:
- Solar cycle.
- Geomagnetic cutoff rigidity.
- Altitude.

Our campaign covered cutoff rigiditedes between 5.5 GV and 8.5 GV (total range from 0 to 18 GV). Complements the range [2.5, 4.5] GV measured by Gordon et al (2004), IEEE 51(6).

Correction for solar activity

HENSA High Efficiency Neutron Spectrometry Array

Data from 25/07/2020 to 17/11/2020.

The reference data is the measurement at IFIC (13/10/20 - 16/10/20).

Each NM data is normalized to this period of time (I/Io).

Corrections are < 1%.

NM	Rc (GV)	Site	Solar Mod. Correction
BKSN (5.70 GV, 1700 m)	5.46	IFCA	1.002
	5.81	Astun	0.997
	5.84	LSC	0.992
ROME (6.27 GV, 0 m)	6.52	UPC	0.997
	6.76	UCM	1.001
NANM (7.10 GV, 2000 m)	7.07	OAJ	1.001
	7.34	IFIC	1.000
	7.34	IFIC_van	1.000
ATHN (8.53 GV, 260 m)	8.49	UGR	1.000
	8.55	IAA	1.005

NMDB data on the HENSA 2020 campaign

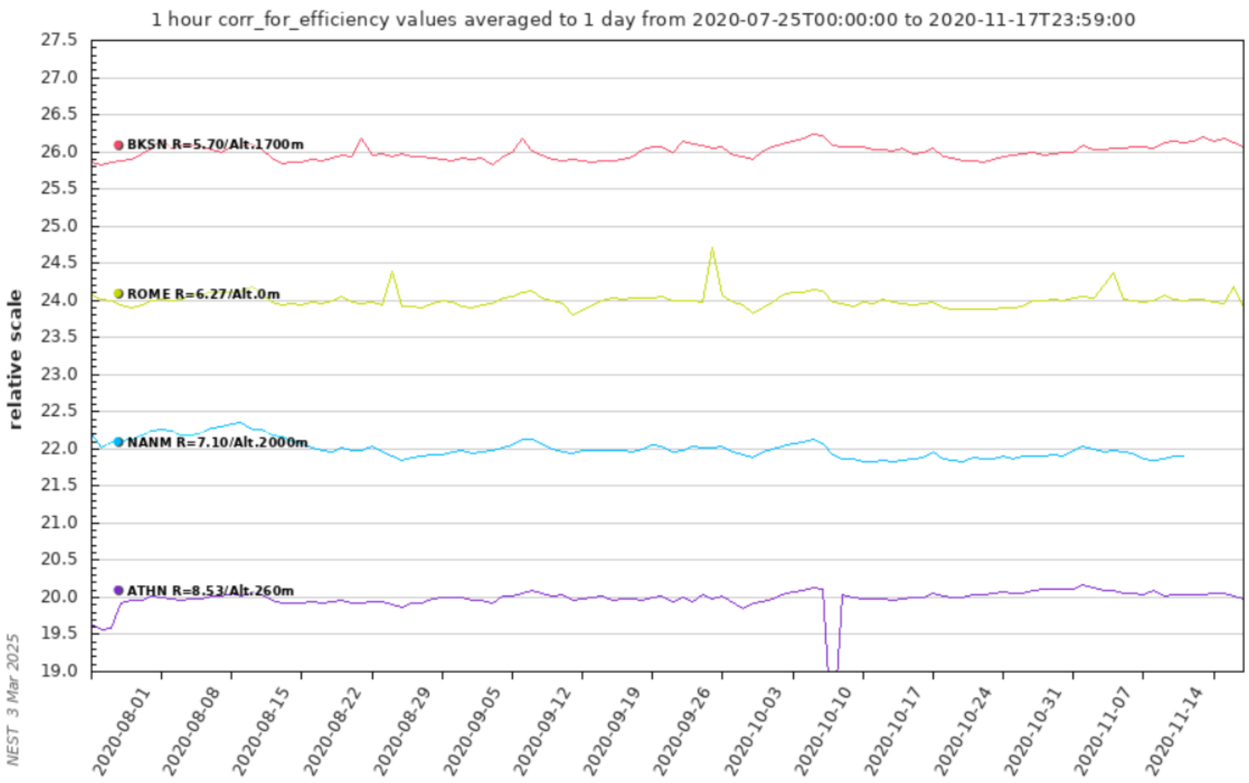

Correction for geomagnetic latitude

HENSA High Efficiency Neutron Spectrometry Array

Correction methodology (> 10 MeV) from Gordon et al. (2004) IEEE 51(6)

$$\frac{d\phi(E)}{dE} = \frac{d\phi_0(E)}{dE} \cdot F_{\text{alt}}(d) \cdot F_{\text{BSYD}}(R_c, d, I)$$

Rc (GV)	Fmin {BSYD}	Fmin/Fific {BSYD}	Solar Mod. Factor
5.46	0.883	1.118	1.002
5.81	0.773	0.979	0.997
5.84	0.810	1.027	0.992
6.52		-	-
6.76	0.788	0.998	1.001
7.07	0.706	0.894	1.001
7.34	0.790	1.000	1.000
7.34	0.790	1.001	1.000
8.49	0.707	0.896	1.000
8.55	0.591	0.748	1.005

IFIC

Correction for altitude

HENSA
High Efficiency Neutron Spectrometry Array

Data corrected by solar modulation and Rc (> 10 MeV)

Then, fitted to the Gordon eq:

$$F_{\mathrm{alt}}(d) = \exp\left[\frac{(d_{\mathrm{SL}} - d)}{L_{\mathrm{n}}}\right]$$

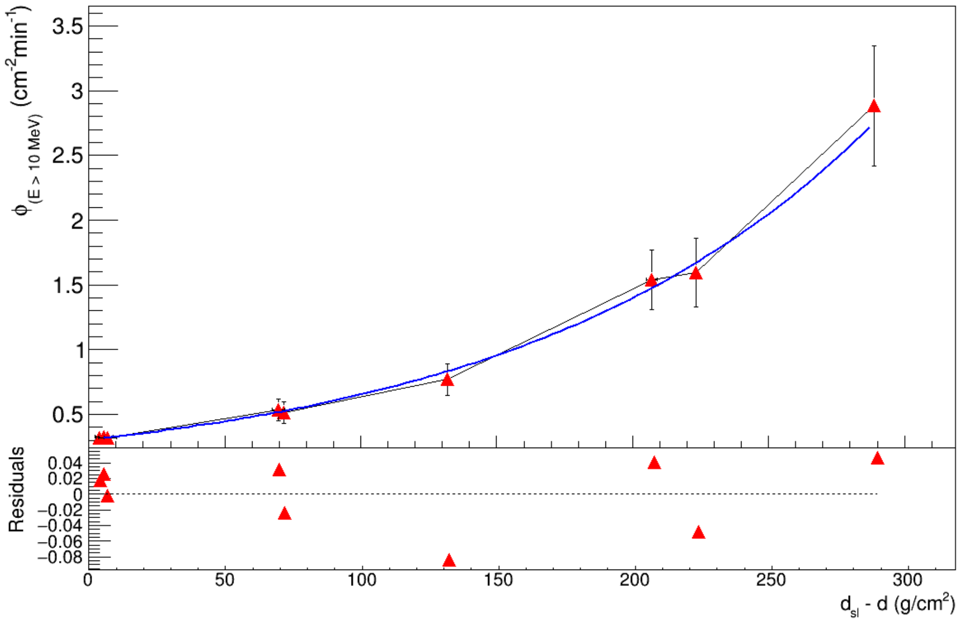

Calculation	Ln (g/cm²)
Gordon et al (2004)	131.3 ± 1.3
This work (2025)	131 ± 9

Unfolding corrected by altitude, SM and Rc

High Efficiency Neutron Spectrometry Array

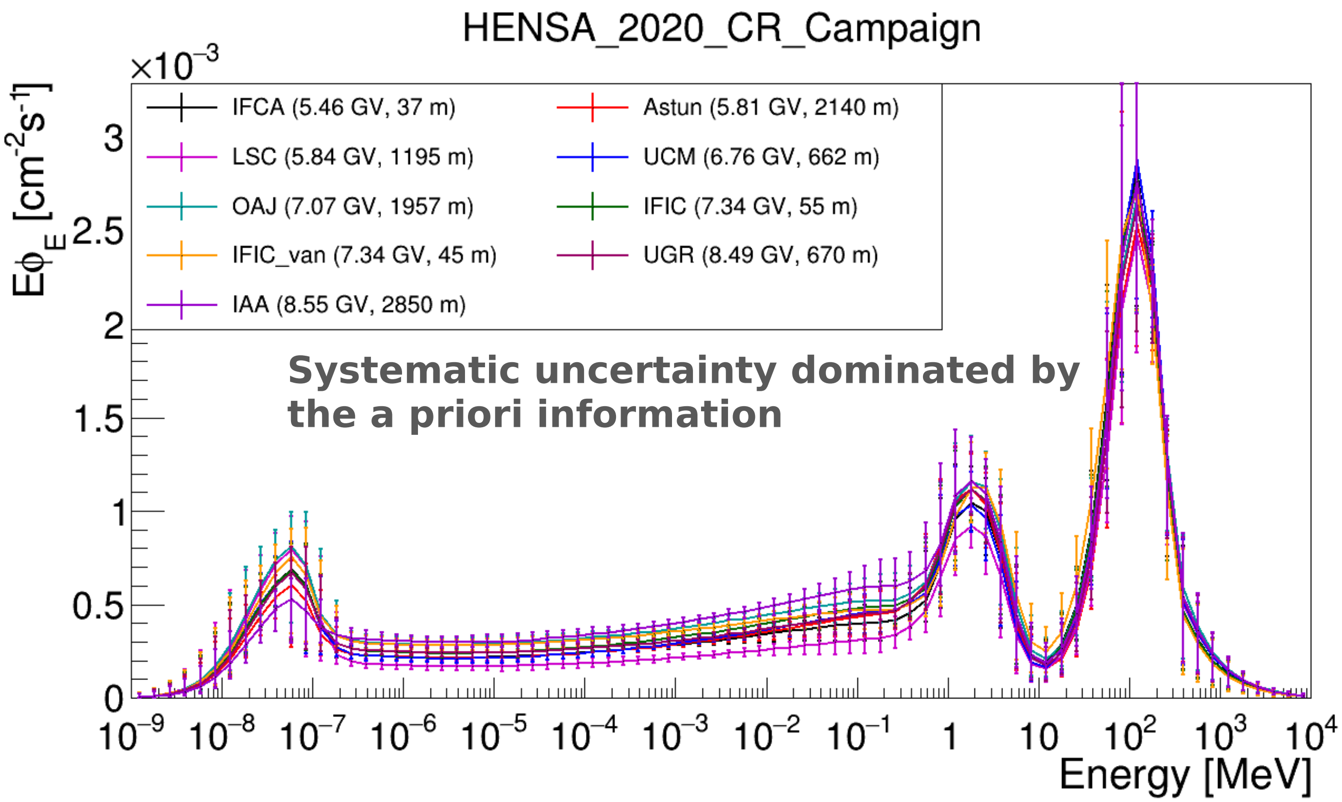

Systematic uncertainty dominated by the a priori information

Integral values

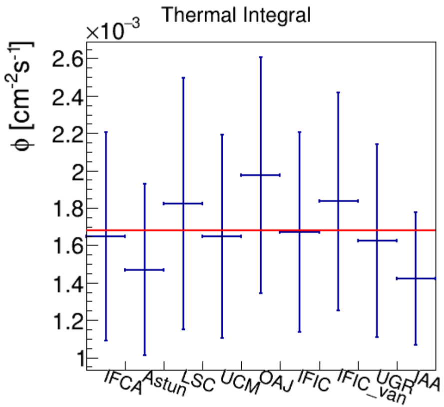

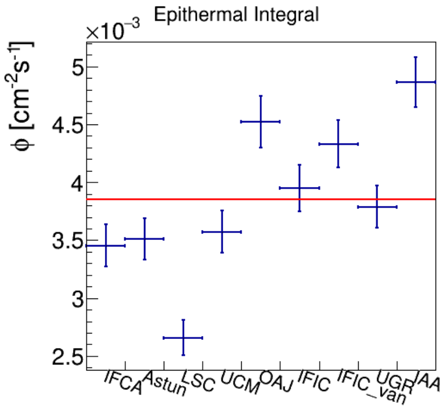

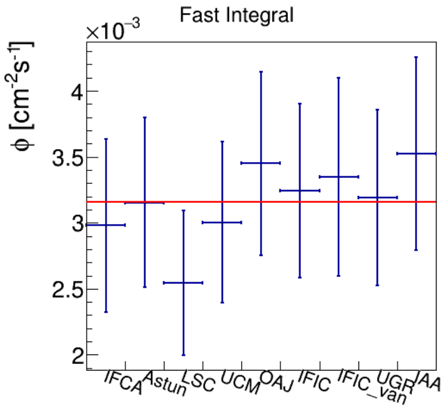

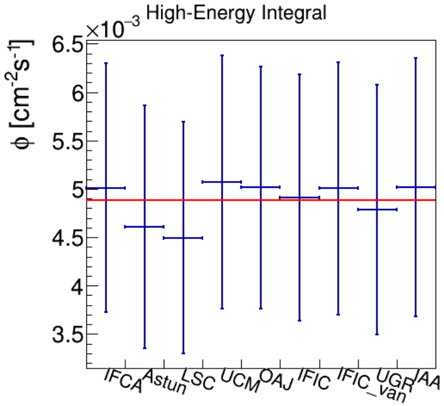

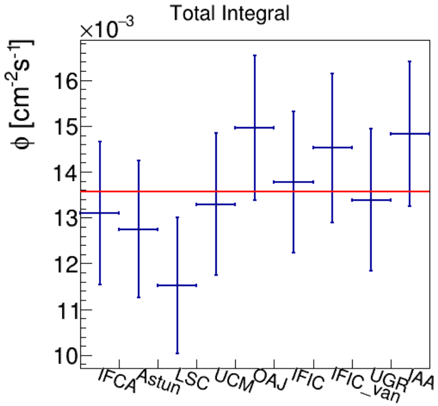

Sorted by Rc

Comparison of the rates uncertainty

Detector	RU in 2h (%)	RU in 1h (%)	RU in 30min (%)
1	1.11	1.67	2.78
2	1.29	1.95	3.18
3	0.93	1.41	2.37
4	0.93	1.40	2.35
5	1.13	1.72	2.87
6	1.34	2.03	3.38
7	1.57	2.36	3.90
8	0.97	1.45	2.49
9	2.56	3.96	6.55
10	1.44	2.15	3.55

Unfolding each 1h @IAA

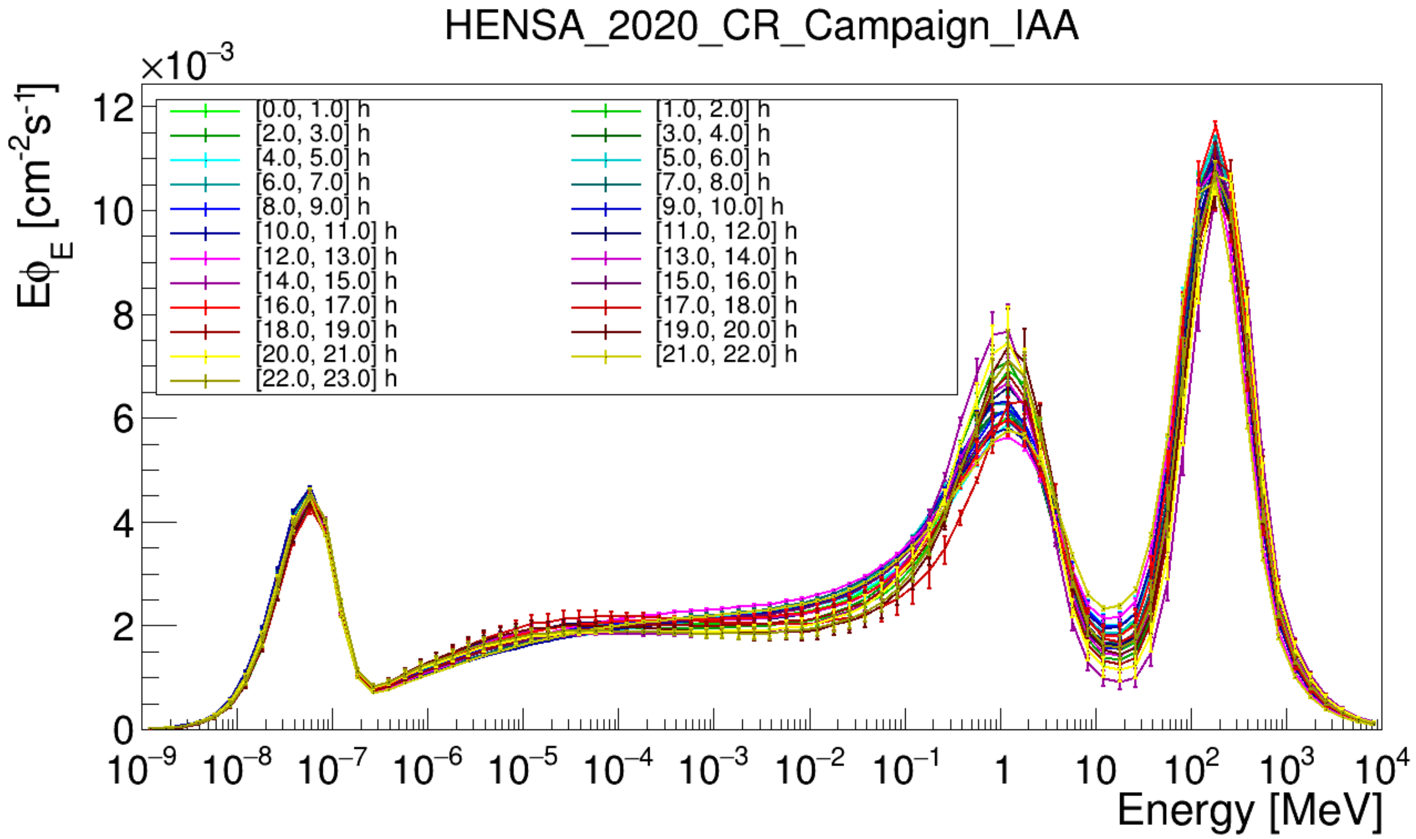

Integrals each 1h @IAA

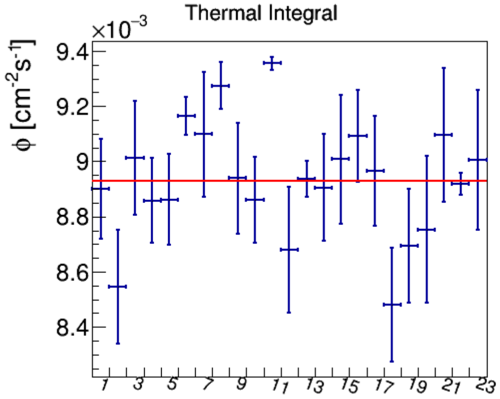

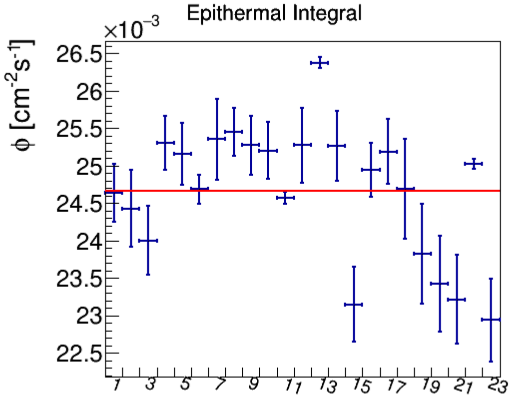

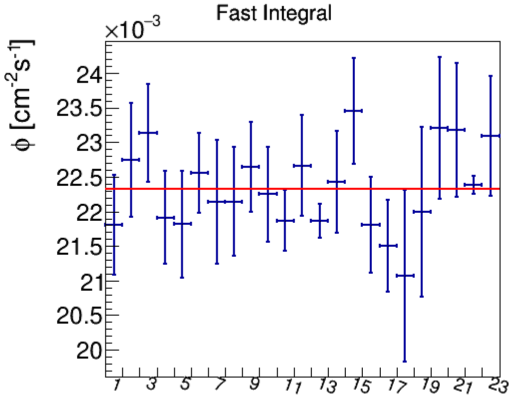

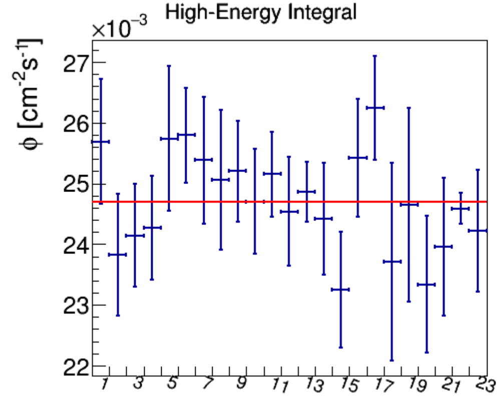

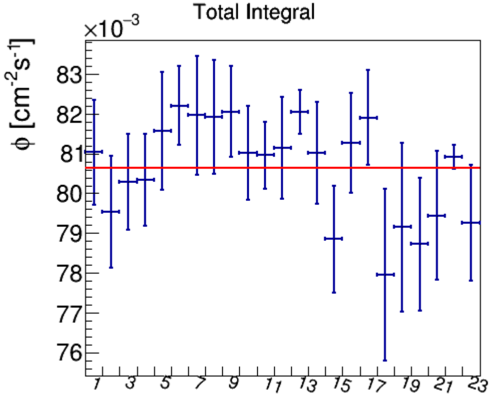

Unfolding each 30min @IAA

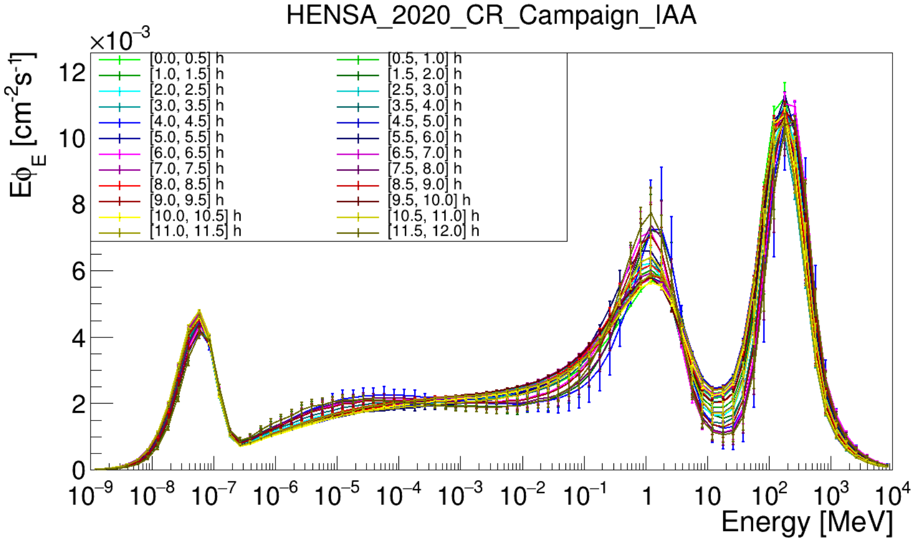

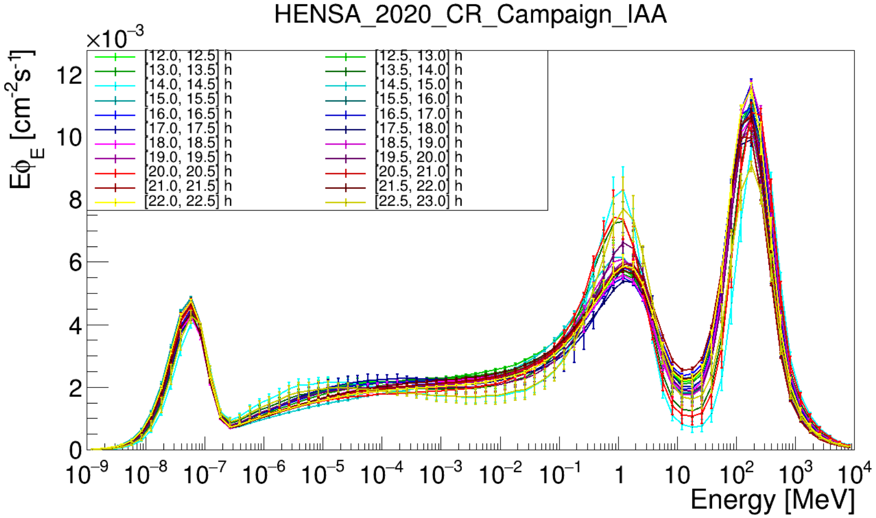

Integrals each 30min @IAA

HENSA
High Efficiency Neutron Spectrometry Array

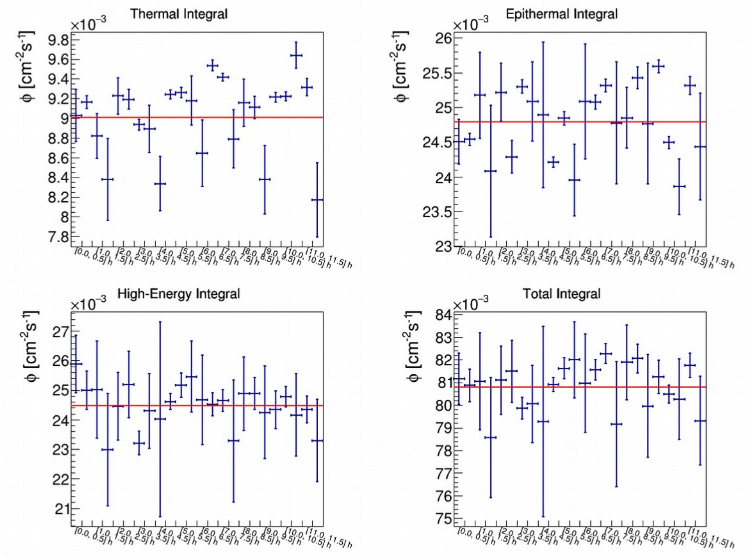

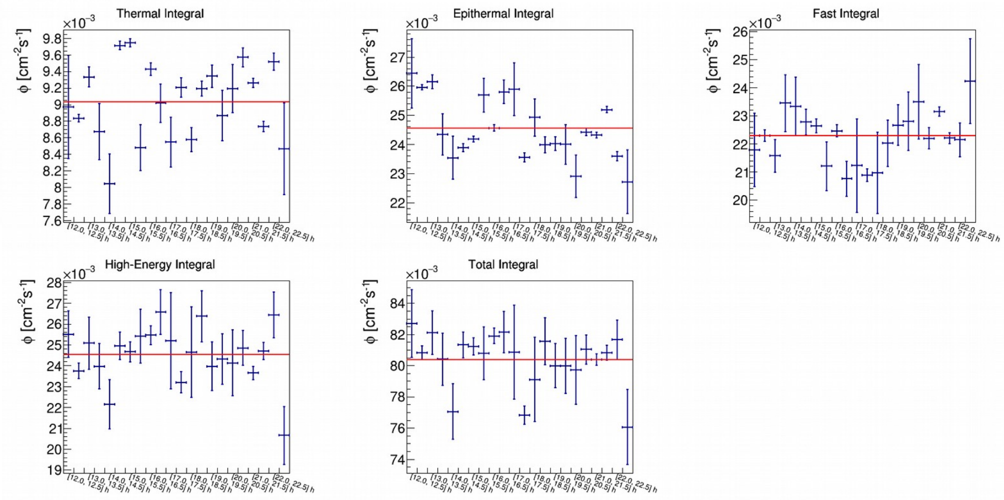

The HENSA++ spectrometer (thesis A. Quero

- HENSA++ is the latest iteration of HENSA (**16 detectors**). During the last 2 years it has been under commissioning.
- Design with **optimized resolution**, overall in the high-energy region.
- Monitor the cosmic-ray neutron spectrum for space weather and ambient dosimetry research.

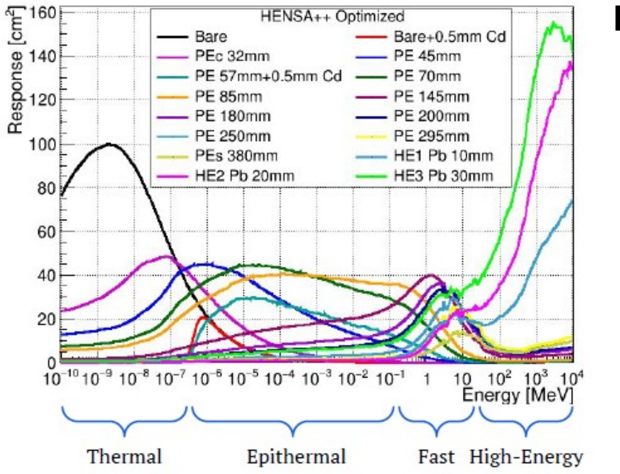

The HENSA++ Response Matrix. Calculated with Geant4.

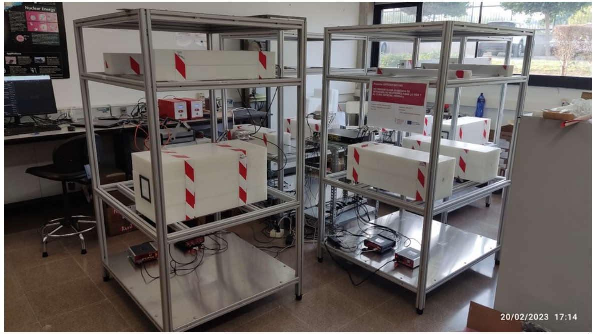

HENSA++ commissioning setup (IFIC Gamma & Neutron Lab)

HENSA++ first outdoors measurement (Zaragoza, Spain)
HENSA – IAXO collaboration

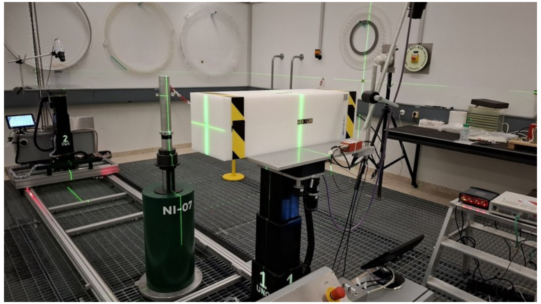

HENSA++ benchmarking exercise with AmBe neutron source (PSI, Switzerland)

The HENSA++ spectrometer at OAJ

HENSA++ Space weather & Dosimetry

HENSA++ at OAJ (Teruel) for space weather applications (since July 2025).

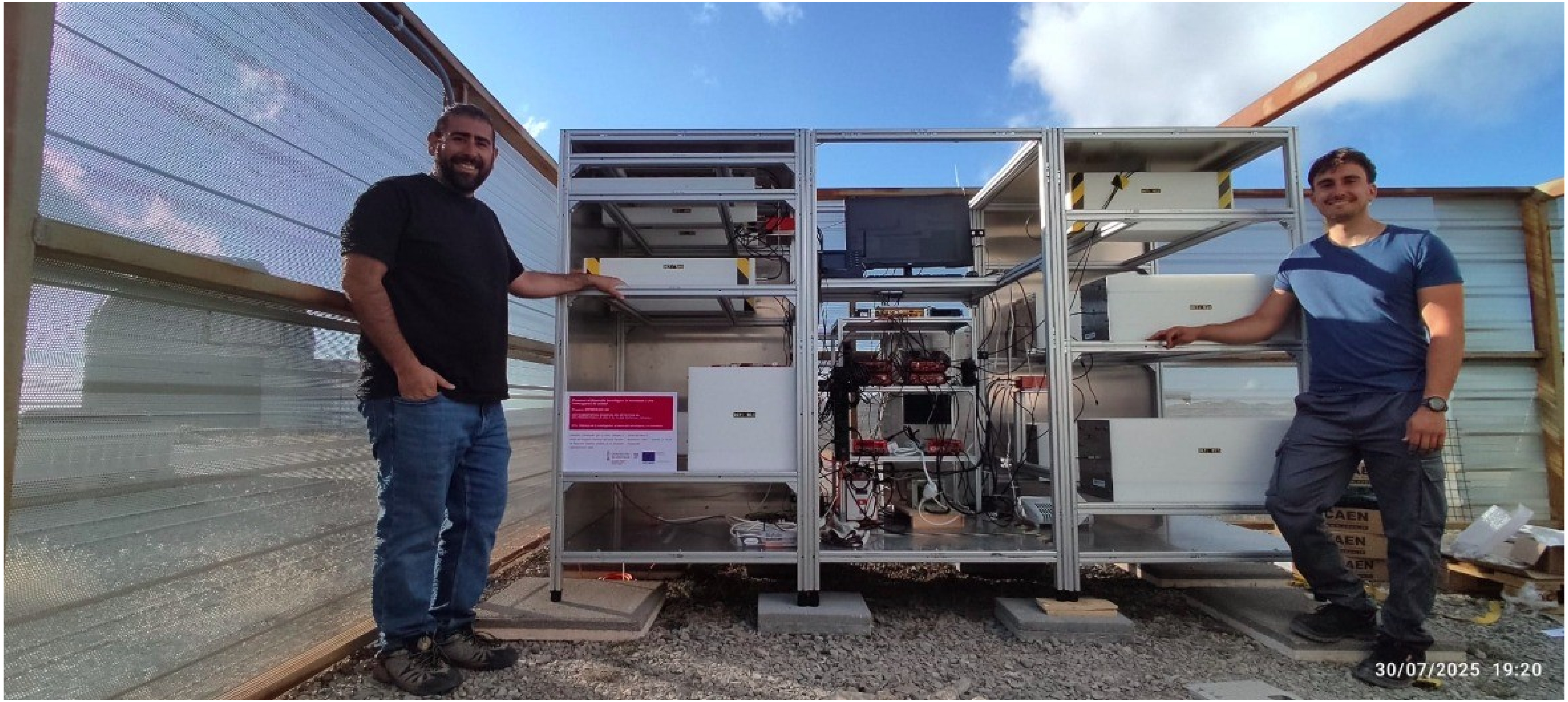

The HENSA++ spectrometer at DESY

HENSA++ Space weather & Dosimetry

HENSA++ for astroparticle physics applications at ground level

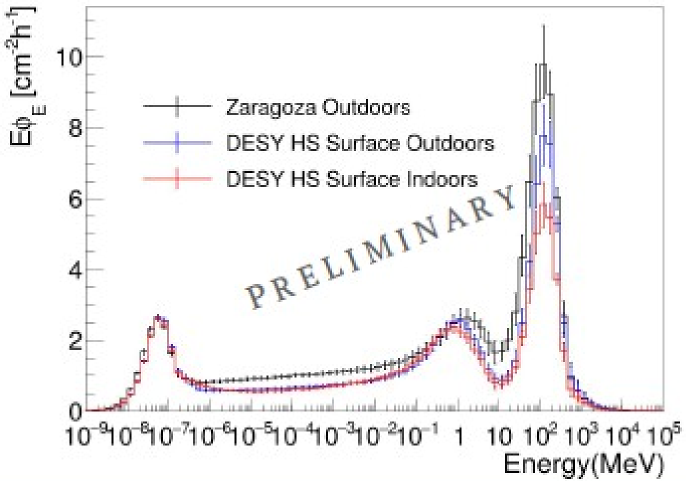

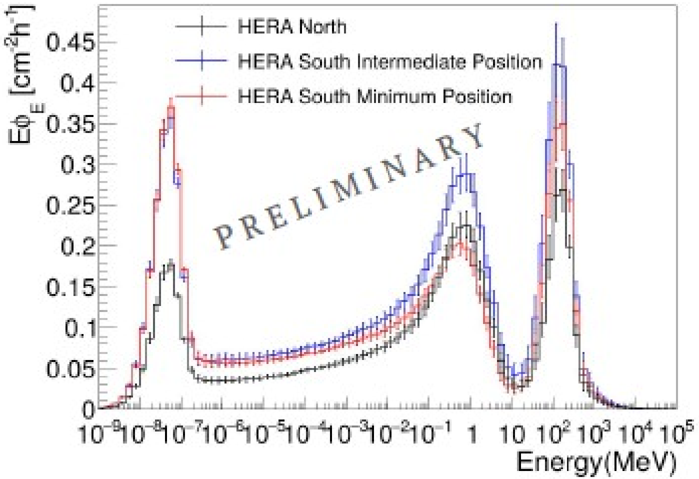

- Unfolding performed with our deconvolution algorithm POU
- Reduction of a 20-30% in the DESY (H ~ 0 masl, Rc = 2.59 GV, June 2025) integral fluence values comparing with Zaragoza (H ~ 200 masl, Rc = 6.22GV, March 2024) . Similar shape.
- Reduction of approximately one order of magnitude in the total fluence when moving underground.

A. Quero-Ballesteros | 22nd IAXO Collaboration Meeting, Dortmund, Germany | 17/09/2025| 13

Final remarks

- The HENSA project provides complementary spectral sensitivity to the NMDB, enhancing the analysis of primary cosmic-ray impacts on Earth.

- In 2020 we have characterized the cosmic-ray neutron spectrum across a broad range of magnetic rigidities. Demonstration of the reconstruction capabilities in time intervals of 30 minutes.

- **Today**: the HENSA++ (update of HENSA) detector has been successfully commissioned at OAJ (Teruel), showing consistency with NMDB measurements and effectively detecting recent solar events. Operating since the end of 2024 (**A. Quero PhD thesis**).

- **Today**: HENSA++ collaboration with IAXO at DESY (**A. Quero PhD thesis**)

- **Future**: space weather studies with HENSA++@OAJ and new spectrometer for collaboration with astroparticle physics experiments (IAXO, CONUS) and others ...

HENSA-CR2020 and HENSA++ collaboration

- UPC: N. Mont-Geli, M. Pallàs, G. Cortés, A. Casanova, P. Calviño, R. Garcia, A. de Blas, B. Brusasco.
- IFIC: A. Tarifeño-Saldivia, J.L. Tain, E. Nache, B. Rubio, C. Domingo, J. Lerendegui, J. Agramunt, S. Orrigo, A. Algora, V. Babiano, J. Balibrea.
- UCM: L.M. Fraile, V. Martínez.
- UGR: A. Quero-Ballesteros, A. Lallena.
- HZDR: D. Bemmerer, M. Grieger.

2020 campaign collaborators: IFCA, IAA, OAJ, LSC, Astún Ski Resort,
HENSA++ collaborators: OAJ, CAPA (UNIZAR), IAXO collaboration, CONUS collaboration

UNIVERSITAT POLITÈCNICA DE CATALUNYA BARCELONATECH
Institut de Tècniques Energètiques

HZDR
HELMHOLTZ ZENTRUM DRESDEN ROSSENDORF

UNIVERSIDAD DE GRANADA

UNIVERSIDAD COMPLUTENSE MADRID

IFIC
INSTITUT DE FÍSICA CORPUSCULAR

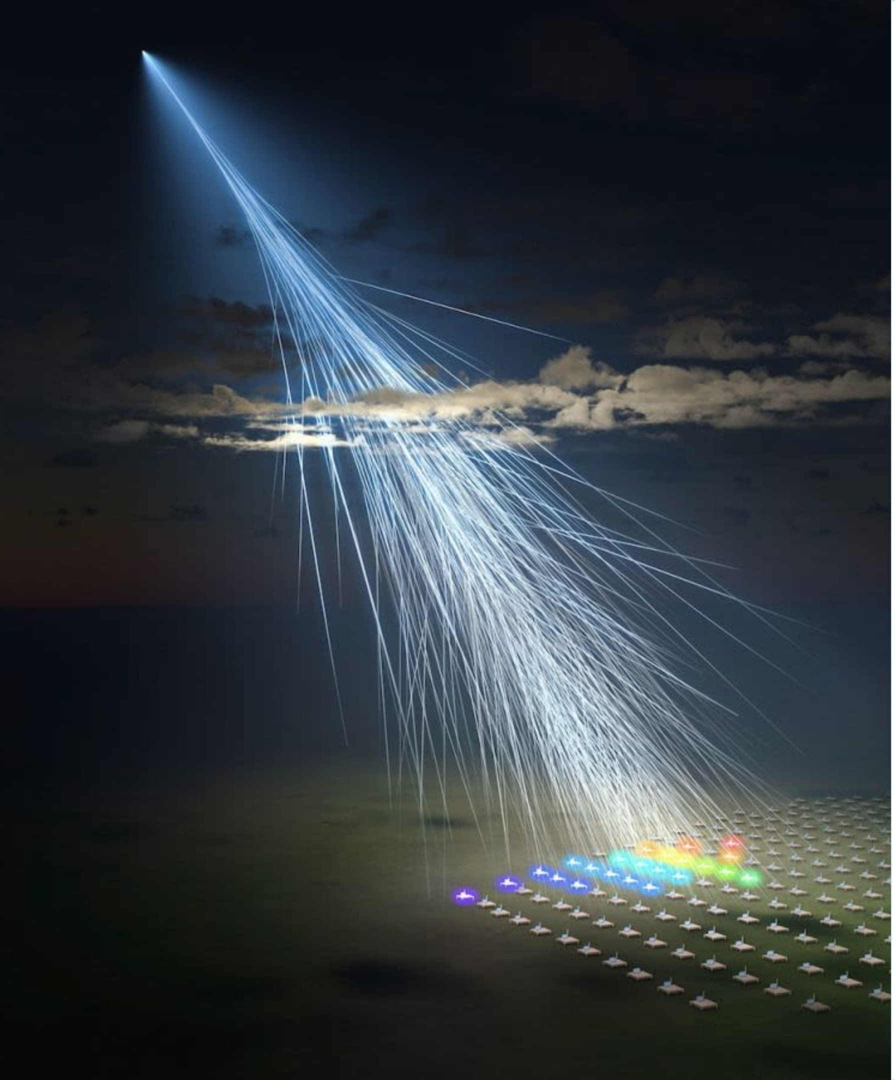

HENSA
High Efficiency Neutron Spectrometry Array

Thank you for your attention!

HENSA++
Space weather & Dosimetry

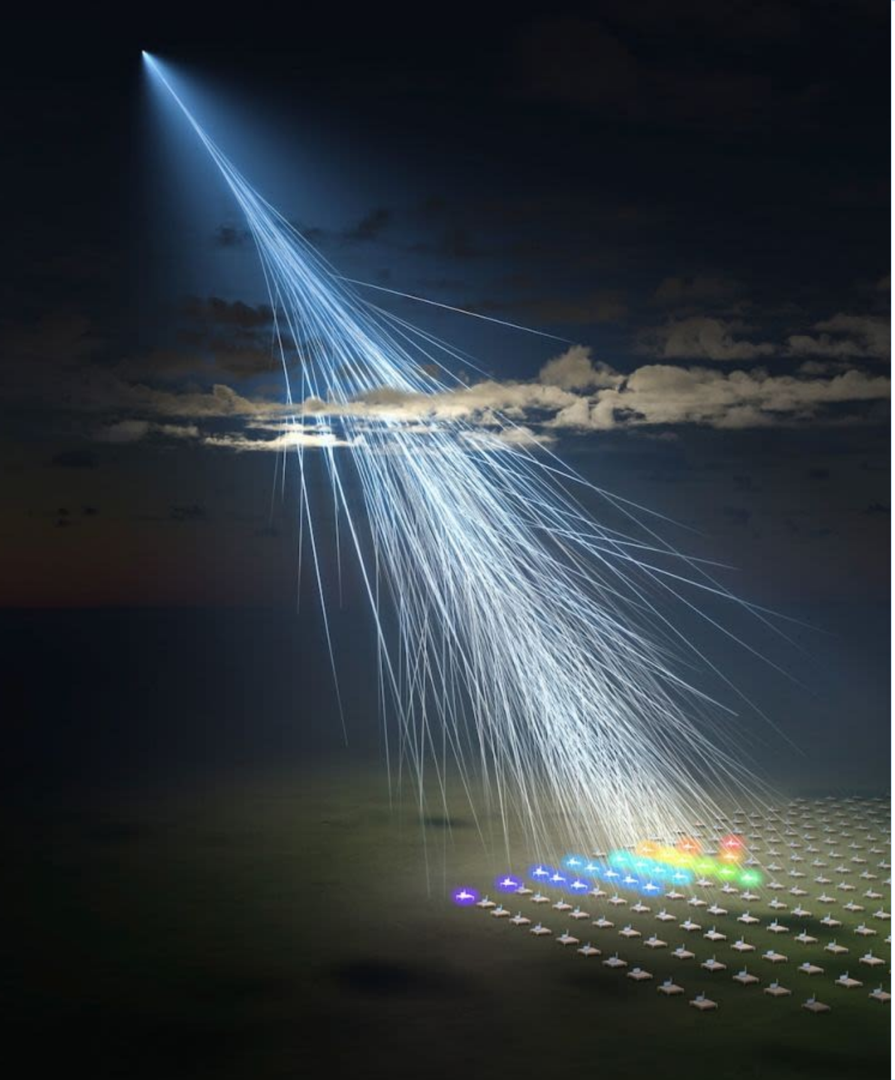

Backup

The 2020 CR campaign

Measurements in nine locations, from Granda to Santander

- Two-three days of acquisition in each location.
- Good statistical resolution (1% to 7%) in 1 hour periods.
- Environmental variables (pressure, temperature, humidity) monitored during the measurement.
- Assume constant flux during the measurements: define an average rate + uncertainty accounting for the fluctuations.

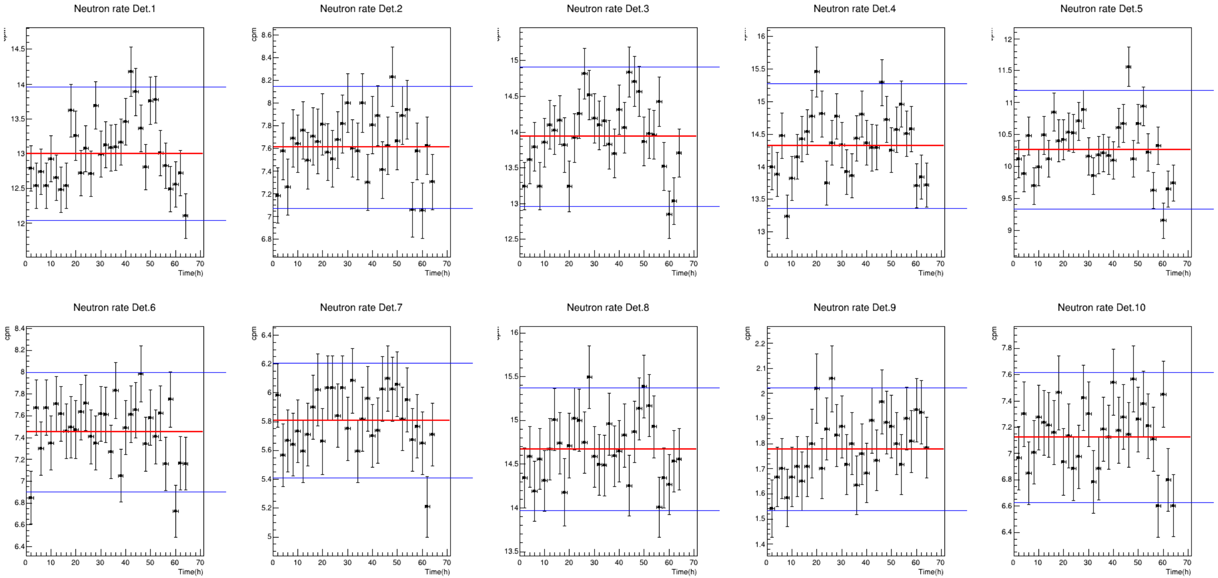

POU Space of parameters

```
####################################################################################################################################

                                            [ G E N E R A L ]

NAME        HENSA_2020_CR                 # Extra label for the output filename.
NPRIORS

####################################################################################################################################

                                          [ E P I T H E R M A L ]

IS          TRUE                            # For activate or deactivate epithermal (TRUE | FALSE)
START       FREE    2.5e-8      7.5e-8      # Start of the function
END         FREE    1.0e+0      3.0e+0      # End of the function
SHAPE       FREE    -0.025      +0.025      # Parameter "b" of the epithermal [-0.05, 0.05]

                                            [ A R T I F A C T ]

IS          FALSE                           # For activate or deactivate artifact (TRUE | FALSE)
POS         FIXED   1.0e-4      1.0e-5      # Central position of the artifact
WID         FIXED   4.0         4.0         # STD in energy decades

####################################################################################################################################

                                             [ P E A K - 1 ]

TYPE        MAXWELL                         # Type: MAXWELL, GAUSS, WATT
PAR_1       FREE    1e-8     1e-7           # Parameter 1 of the peak
PAR_2       FREE    1.00     3.0            # Parameter 2 of the peak

                                              [ P E A K - 2 ]

TYPE        MAXWELL                         # Type: MAXWELL, GAUSS, WATT
PAR_1       FREE    1.00     5.00           # Parameter 1 of the peak
PAR_2       FREE    1.00     3.0            # Parameter 2 of the peak

                                              [ P E A K - 3 ]

TYPE        MAXWELL                         # Type: MAXWELL, GAUSS, WATT
PAR_1       FREE    50       150            # Parameter 1 of the peak
PAR_2       FREE    1.00     3.0            # Parameter 2 of the peak

####################################################################################################################################
```

Solar modulation of the primary spectrum

Solar Minimum

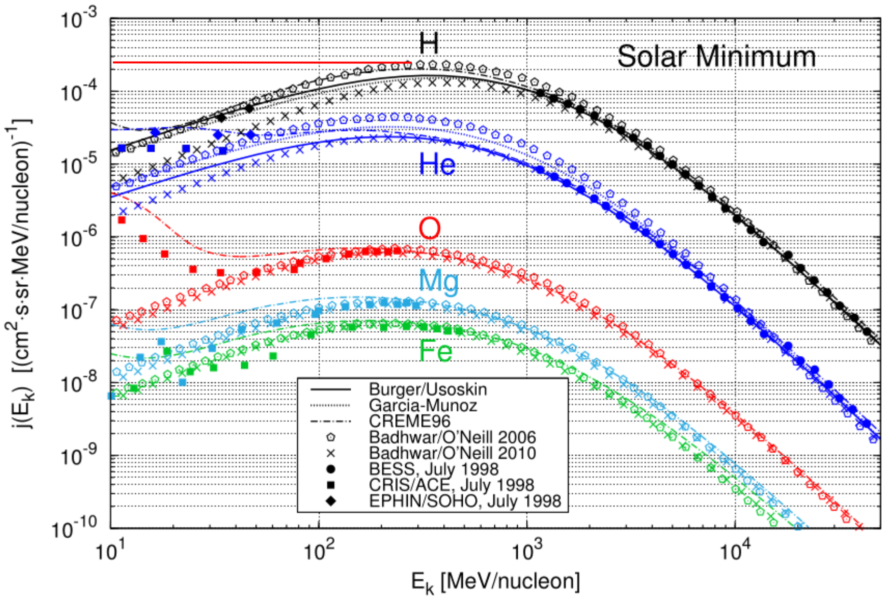

Solar Maximum

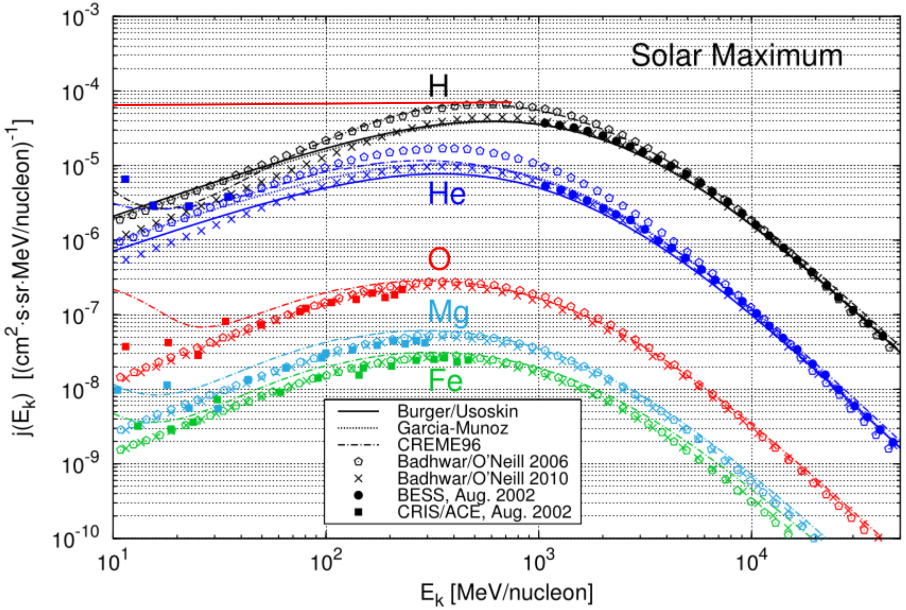

Differential particle intensities of primary galactic H, He, O, Mg, and Fe ions as a function of kinetic energy per nucleon measured near Earth during the BESS experiments (Sanuki et al., 2000; Haino et al., 2004), with the CRIS detector on-board ACE (Stone et al., 1998; Haino et al., 2004), and with EPHIN on-board SOHO (Müller-Mellin et al., 1995) in July 1998 (top panel), i.e. solar minimum, and Augus 2002 (bottom panel), i.e. solar maximum conditions. Experimental data are compared with predictions using models of Burger/Usoski (Burger et al., 2000; Usoskin et al., 2005), Garcia-Munoz (Garcia-Munoz et al., 1975), CREME96 (Tylka et al., 1997), and Bad-hwar/O'Neill (O'Neill, 2006, 2010). Pioch PhD Thesis (2012)

Behaviour of charged particles in the Earth magnetic field

The Earth magnetic field acts as a shielding against cosmic-rays

$$R = \frac{pc}{|q|} = \frac{pc}{Ze} = r_L|\vec{B}|c$$

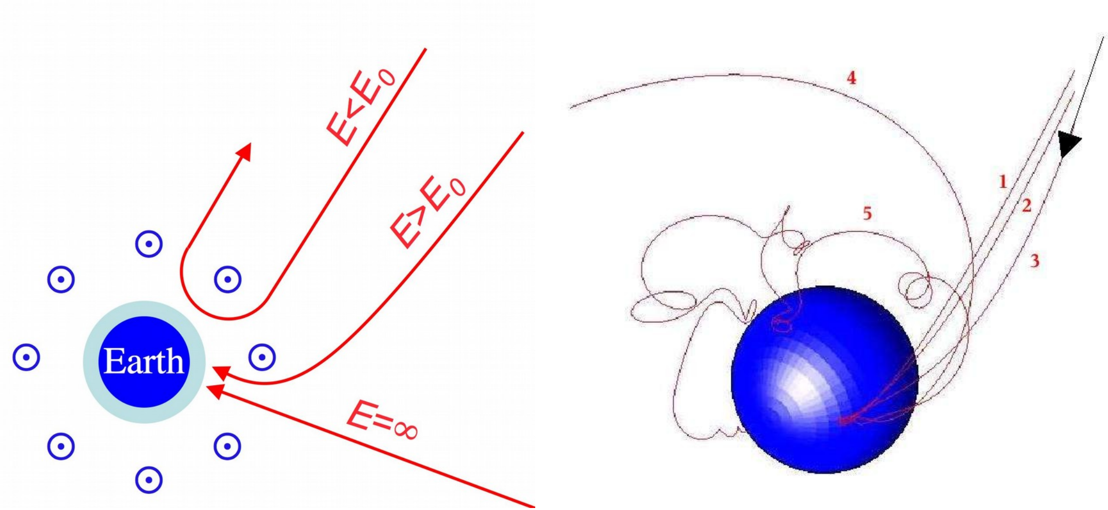

Trajectories of charged particles in the Earth magnetic field. From: https://www.nmdb.eu/public_outreach/es/03/

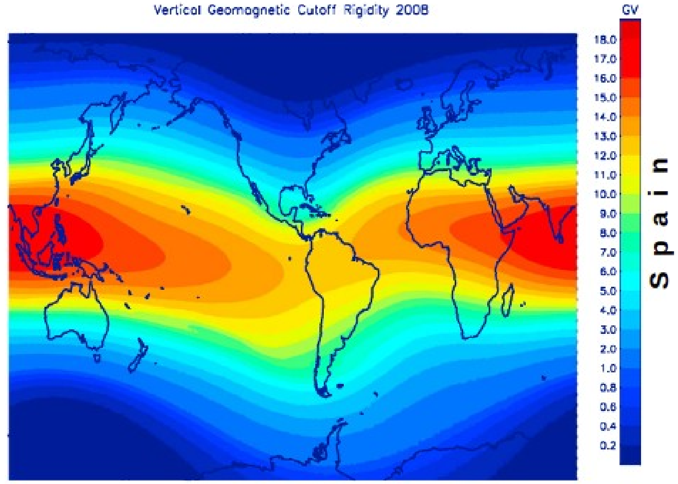

Figure 3. Global grid of vertical geomagnetic cutoff rigidities (GV) calculated from charged particle trajectory simulations in the IGRF field for 2008.

The origin of background neutrons

At surface level

Nuclear cascade reactions generated by primary cosmic-rays (p^+, He)

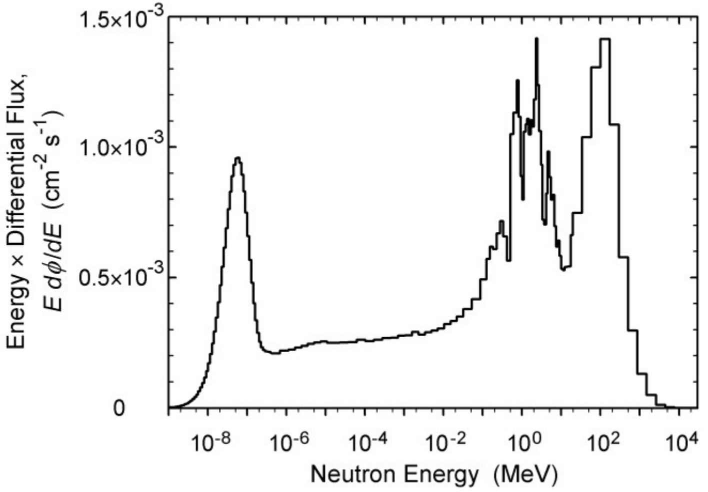

Measured cosmic-ray neutron spectrum on Yorktown Heights, NY. Gordon et al (2004), IEEE 51(6)

In underground laboratories

- (α, n) reactions on rocks
- Spontaneous Fission (U/Th)
- Neutrons induced by cosmic muons

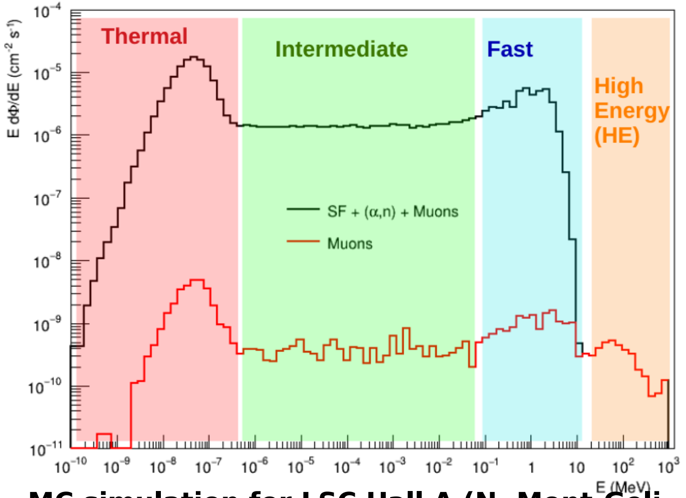

MC simulation for LSC Hall A (N. Mont-Geli, UPC)

HENSA setup: “active part”

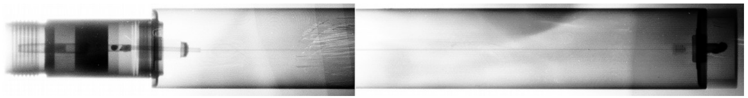

Detection reaction:

$$^3He + n \rightarrow {}^3H + p \quad \mathbf{Q=0.764\ MeV}$$

High Thermal cross section!!:
5330b

Table 13-1. Neutron and gamma-ray interaction probabilities in typical gas proportional counters and scintillators

Thermal Detectors	Interaction Probability: Thermal Neutron	Interaction Probability: 1-MeV Gamma Ray
^{3}He (2.5 cm diam, 4 atm)	0.77	0.0001
Ar (2.5 cm diam, 2 atm)	0.0	0.0005
BF_3 (5.0 cm diam, 0.66 atm)	0.29	0.0006
Al tube wall (0.8 mm)	0.0	0.014
Fast Detectors	**1-MeV Neutron**	**1-MeV Gamma Ray**
^{4}He (5.0 cm diam, 18 atm)	0.01	0.001
Al tube wall (0.8 mm)	0.0	0.014
Scintillator (5.0 cm thick)	0.78	0.26

*Extracted from Neutron Detectors, T. W. Crane and M. P. Baker

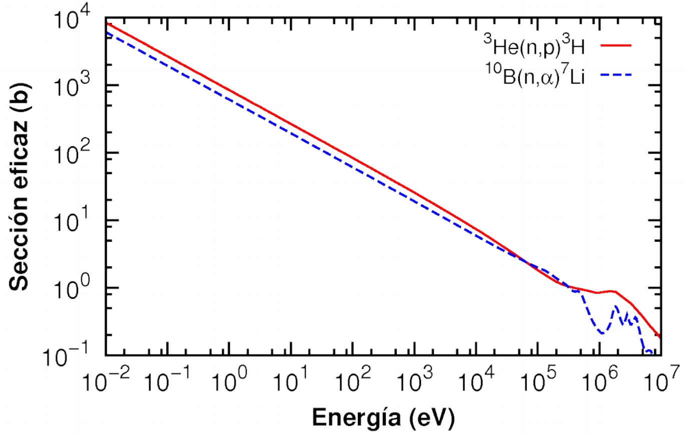

- These neutron counters are gaseous ionization detectors that use 3He as converting gas.
- Due to the high thermal capture cross section, 3He filled counters have a high neutron sensitivity.
- For non-thermal neutrons, the high efficiency can be exploited by using moderators.
- In addition, the low gamma-ray sensitivity makes these detectors very attractive for neutron spectroscopy (Bonner spheres).

HENSA comparison with BSS

Standard extended Bonner Spheres

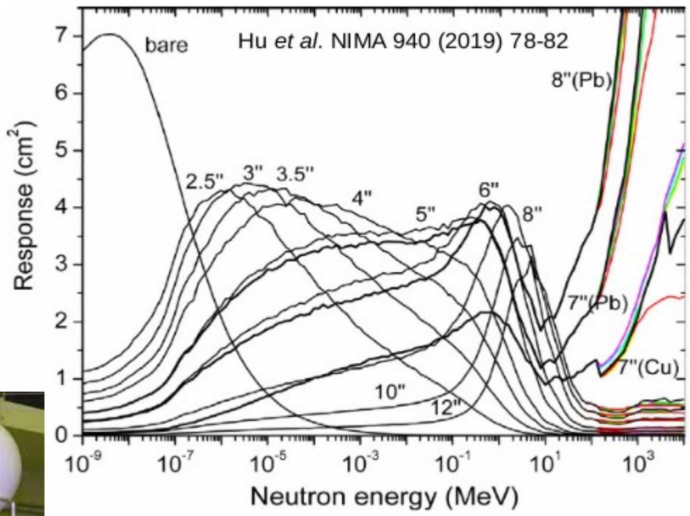

HENSA 2019 version

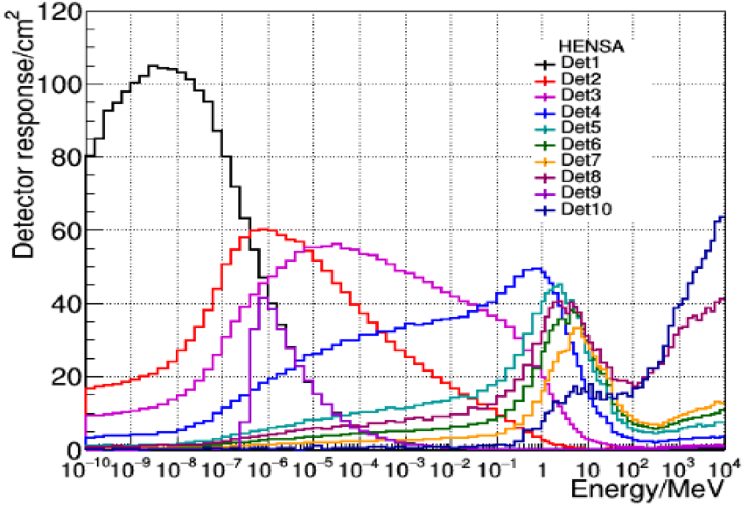

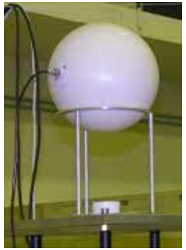

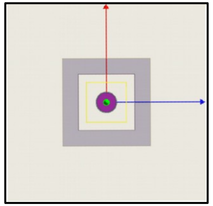

- HENSA neutron response is **5-15** times greater than standard BSS thanks to the increase in the detector active length
- The change in the topology is not a problem in isotropic fields

Optimization of HENSA++: Resolving power kern

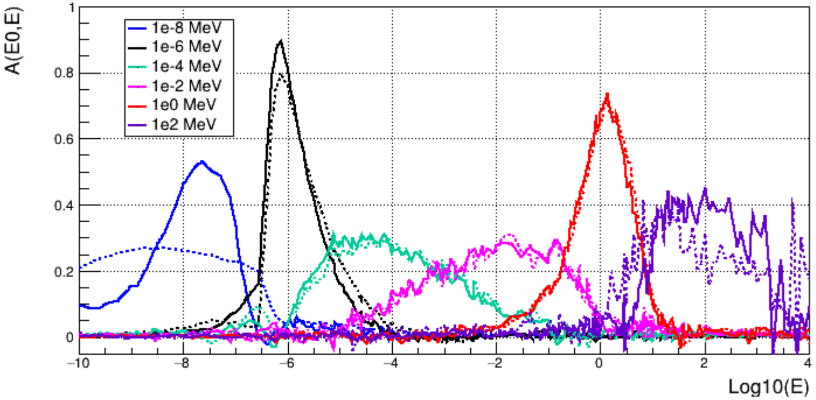

Dotted: Initial | Continuous: Optimized

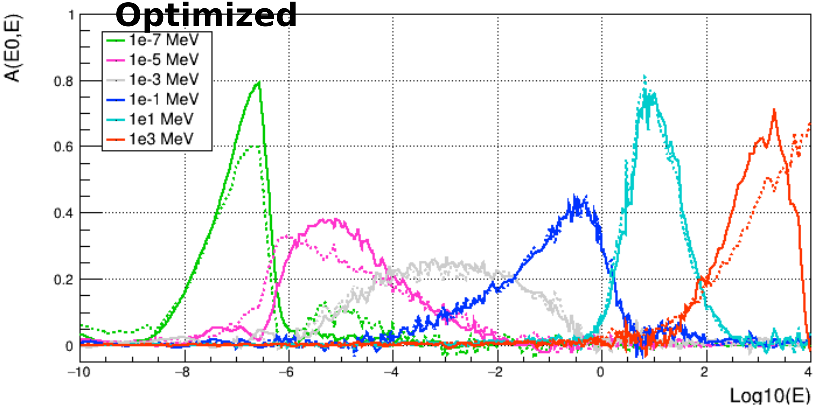

LogE	Mean(vInit)	Mean(vOpt)	SD(vOpt)/SD(vInit)-1
-8	-7.72	-7.69	-44.20%
-7	-6.76	-6.86	-51.11%
-6	-5.76	-5.89	-20.37%
-5	-4.93	-4.86	-24.11%
-4	-3.93	-3.98	-4.65%
-3	-3.00	-2.98	-8.27%
-2	-2.07	-2.08	-2.13%
-1	-1.12	-1.09	2.56%
0	-0.08	-0.09	-1.71%
1	0.91	0.94	-2.15%
2	1.43	1.72	-38.90%
3	2.71	2.73	-39.72%

ELSEVIER

Nuclear Instruments and Methods in Physics Research A 480 (2002) 690–695

NUCLEAR INSTRUMENTS & METHODS IN PHYSICS RESEARCH Section A

www.elsevier.com/locate/nima

Resolving power of a multisphere neutron spectrometer

Marcel Reginatto*

$$< \phi >_{E_0} = \int A(E_0, E)\phi(E)dE$$

Unfolding Parametric codes

- Parametric codes: Model the neutron spectrum based on the physics of neutron interactions (e.g., MITOM, FRUIT).
- They generate multiple spectra using Monte Carlo sampling and select the one that best fits the data by minimizing the chi-squared value.

$$\chi^2 = \frac{1}{n}\sum_{i=1}^{n}\left(\frac{C_i^{input} - C_i^{output}}{\sigma_i^{input}}\right)^2$$

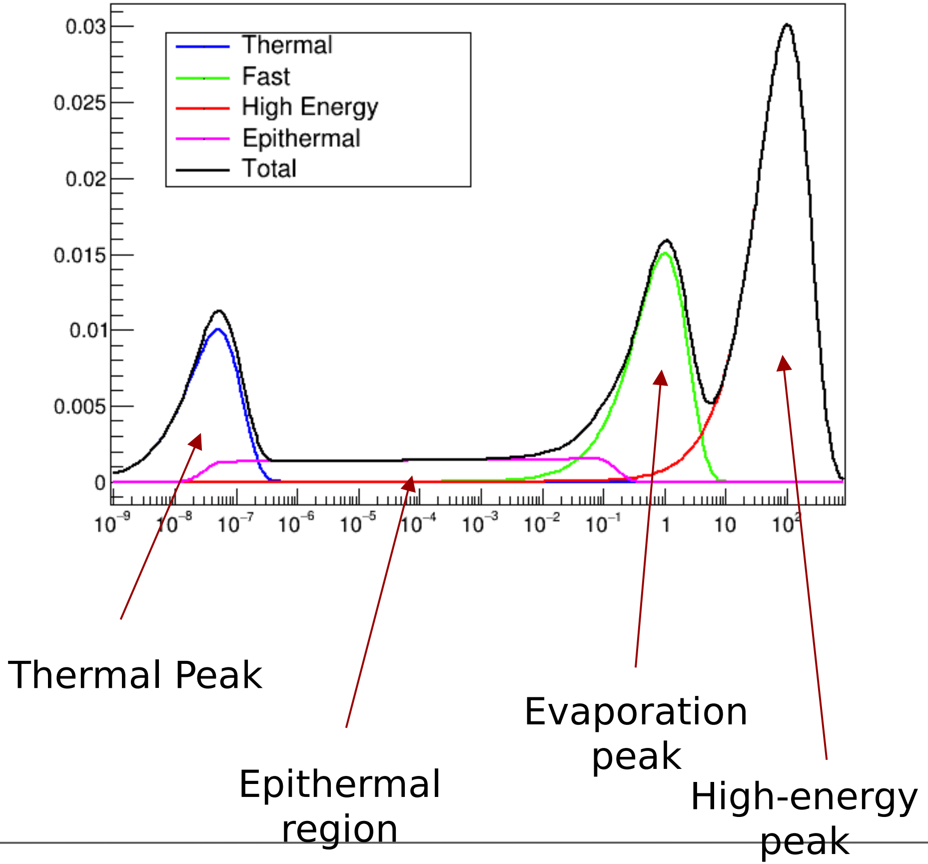

Unfolding Iterative codes

- Iterative codes: Employ some “a priori” spectrum and perturb it iteratively based on mathematical algorithms (eg. MAXED, GRAVEL, BAYES)
  - Entropy maximization (Information Theory)

    $$\text{max:}\ \ S[\mathbf{f}] - \frac{1}{\lambda}\chi^2[\mathbf{f}] \qquad S[\mathbf{f}] = -\sum_{i=1}^{n}\left(f_i \ln\frac{f_i}{h_i} - f_i + h_i\right)$$

  - Expectation maximization (Bayes Theorem)

    $$\hat{f}_j = \frac{1}{\sum_{i=1}^{n} R_{ij}} \sum_{i=1}^{n} P(f_j|d_i)\hat{d}_i, \quad j = 1,\ldots,m$$

These codes iterate until some stopping criteria is reached. Usually, chi-squared:

$$\chi^2 = \frac{1}{n}\sum_{i=1}^{n}\left(\frac{C_i^{input} - C_i^{output}}{\sigma_i^{input}}\right)^2$$

$$\chi^2 \approx 1$$

Recent activities with HENSA++ at the Paul Scherrer Institute (PSI)

Intercomparison exercise BSS measurements
(p-channel, Target M)

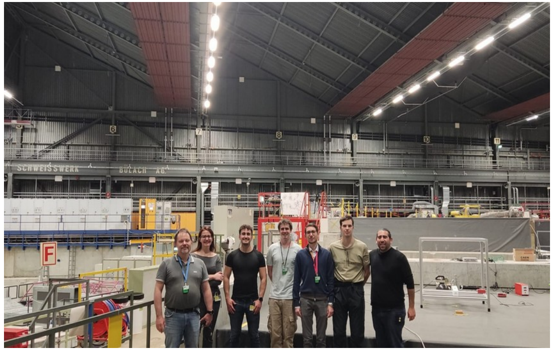

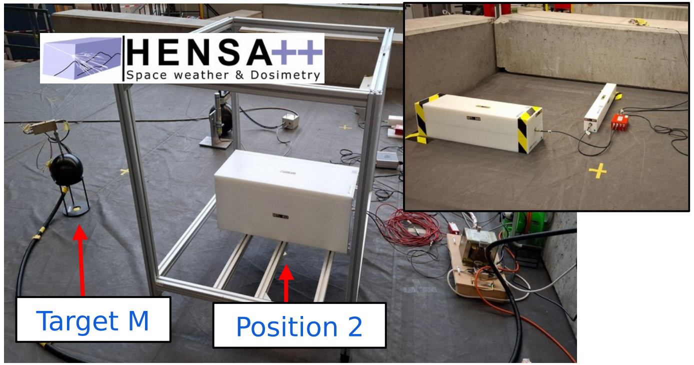

Benchmarking measurements with AmBe source
(Calibration laboratory)

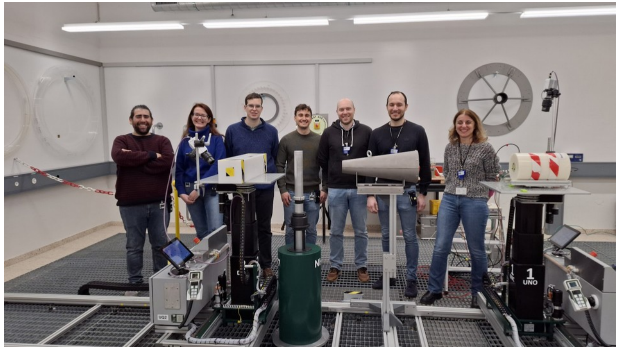

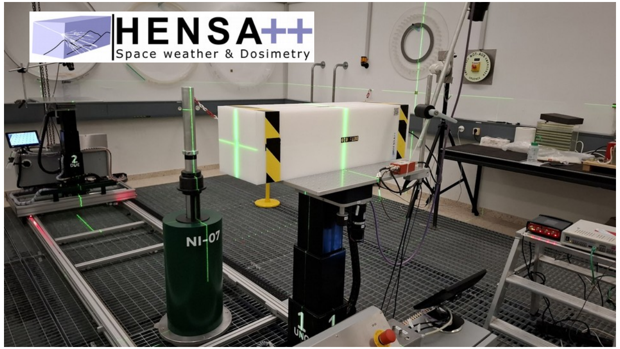

Applications: Underground (I)

HENSA
High Efficiency Neutron Spectrometry Array

HENSA at Felsenkeller, Germany (2020)

M Grieger et al (2020), Phys Rev D, 101, 123027

HENSA at LSC Hall A, Spain (2020)

SEA Orrigo et al (2022), Eur Phys Journal C, 82, 814

Applications: Underground (II)

HENSA at LSC Hall B, Spain (Since 2021)

N Mont-Geli et al (2023), Proceeding of Science 441, 312

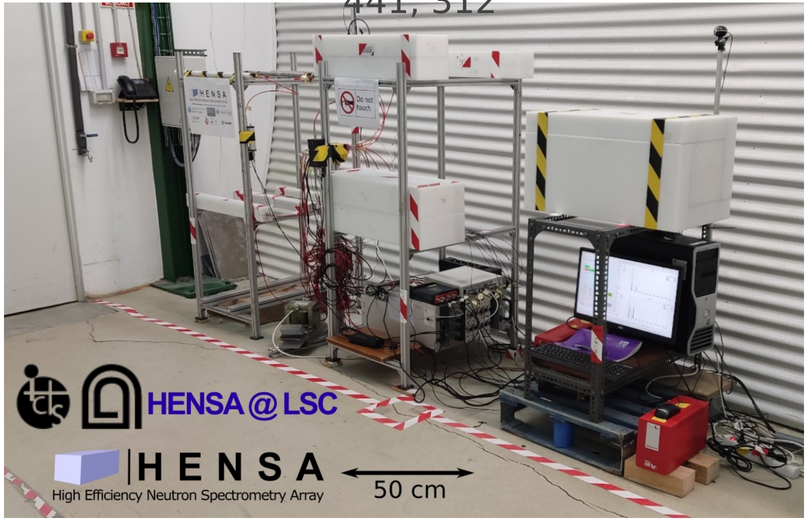

HENSA at LNGS, Gran Sasso, Italy (Since 2024)

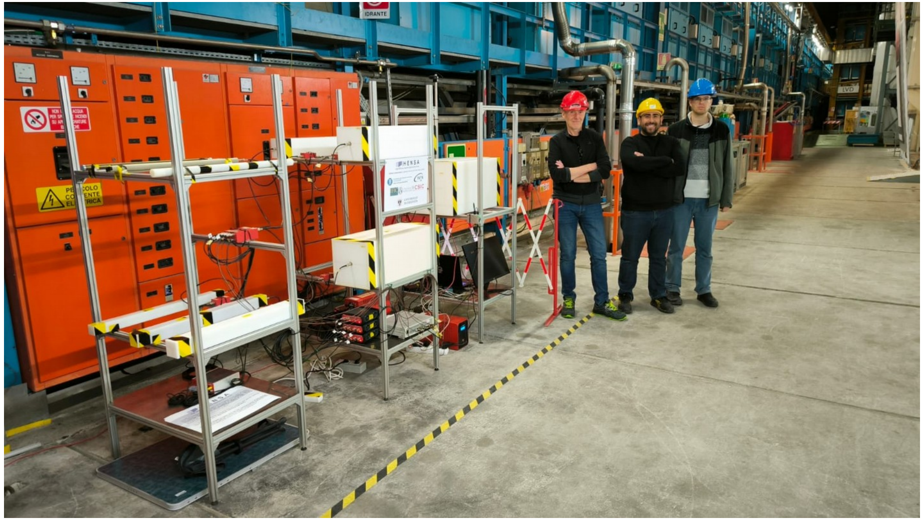

Comparison of each channel with meteo data

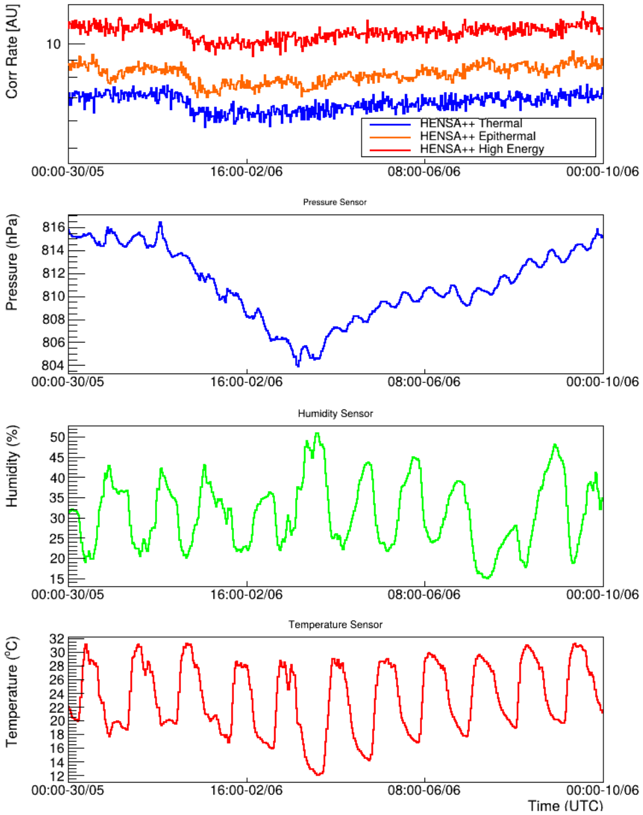

GSE coordinate system